

## First results from the LHCb experiment

H. GORDON(\*) for the LHCb COLLABORATION

*University of Oxford - Oxford OX1 3RH, UK*

(ricevuto il 20 Luglio 2011; pubblicato online l'8 Ottobre 2011)

**Summary.** — The LHCb experiment is a precision heavy flavour experiment at the Large Hadron Collider. This contribution gives an introduction to the experiment, a short summary of the detector performance, and an overview of selected first results. These first measurements of particle production are set in the context of prospects for precision measurements of Standard Model parameters and searches for new physics.

PACS 13.85.-t – Hadron-induced high- and super-high-energy interactions (energy  $> 10$  GeV).

PACS 14.40.-n – Mesons.

### 1. – Introduction

The LHCb detector is a single-arm spectrometer at the Large Hadron Collider (LHC). The principal objective is to search for new physics indirectly, by looking for deviations from Standard Model values for  $CP$ -violation parameters and in the branching ratios of rare processes. The focus is on measurements of  $b$  and  $c$  quark decays, but there are also initiatives to study top and electroweak physics.

The LHC delivers proton-proton collisions at rates of up to 40 MHz and centre-of-mass energy  $\sqrt{s} = 7$  TeV. The LHCb detector covers the region around the interaction point where the  $b$ -hadron production cross section is highest, at low angles to the beam. The acceptance spans polar angles from 10 to 300 mrad in the vertical and 10 to 250 mrad in the horizontal planes.

To resolve individual particle decays, LHCb has an extremely precise vertex detector (VELO), which moves inwards to within 7 mm of the LHC beam during data taking. There is also a comprehensive particle identification system, which comprises five muon stations, electromagnetic and hadronic calorimeters, and two Ring Imaging Cherenkov (RICH) detectors. These last distinguish kaons from pions and protons for the momentum range of interest between 2 and 100 GeV/ $c$ . The calorimeters and muon stations

---

(\*) E-mail: [h.gordon1@physics.ox.ac.uk](mailto:h.gordon1@physics.ox.ac.uk)

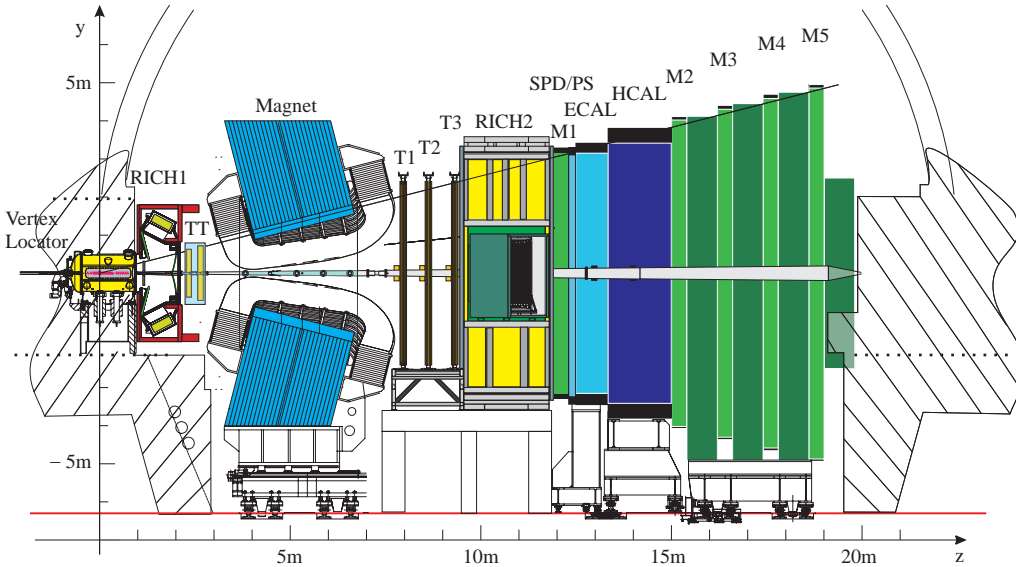


Fig. 1. – The LHCb detector.

also form the backbone of the trigger. The first, hardware stage of the trigger is based on transverse energy, muon ID, and hit multiplicity, and reduces the event rate from the 40 MHz of the LHC clock to 1 MHz. The next two stages of software triggers carry out track reconstruction and reduce the rate further to  $\mathcal{O}(2-3)$  kHz. A diagram of the detector is shown in fig. 1 and further details of the detector can be found in ref. [1].

## 2. – Detector performance

In 2010,  $37 \text{ pb}^{-1}$  of data were collected. Almost all of this was recorded in the last two months of proton-proton running. As the instantaneous luminosity increased, the detector, and especially the trigger, adapted well to a rapidly changing environment. The data were taken with an average number of proton-proton interactions per bunch crossing of up to 2.4, compared to the design value of 0.4. It is foreseen that LHCb will receive of the order of  $1 \text{ fb}^{-1}$  of data in 2011 [2].

The various subdetectors have risen to the challenges presented to them in 2010. After only a few weeks of data taking, the mass resolutions of reconstructed particles were already close to Monte Carlo predictions: for example, the width of the  $\Upsilon$  was 47 MeV in the first  $4 \text{ pb}^{-1}$  of integrated luminosity, compared to 40 MeV in Monte Carlo. The reconstruction of the  $\Upsilon(1S)$ ,  $\Upsilon(2S)$  and  $\Upsilon(3S)$  resonances is shown in fig. 2. The VELO performance can be quantified by the impact parameter resolution, which is also close to that expected from Monte Carlo. This is crucial for separation of  $B$  decays from  $D$  decays. Similarly the RICH mis-identification rates are relatively low and comparable to expectations, and the calorimeters were used successfully to identify neutral particles soon after data taking began. The rapid commissioning of the subdetectors enabled several key physics measurements to be performed during the 2010 run.

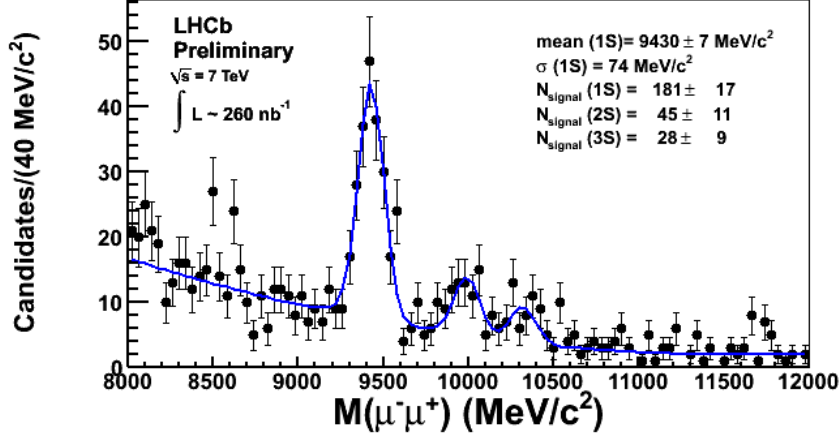


Fig. 2. – Reconstruction of  $\Upsilon \rightarrow \mu^+\mu^-$  decays with  $4\text{ pb}^{-1}$  of LHC data.

### 3. – Prompt $K_S^0$ production

The cross section for  $K_S^0$  particles that come directly from the proton-proton collision was measured in the channel  $K_S^0 \rightarrow \pi^+\pi^-$  using data from the 2009 LHC pilot run at  $\sqrt{s} = 0.9\text{ TeV}$  [3]. Every combination of two oppositely charged intersecting tracks was considered to be a candidate  $K_S^0$ . The measurement of the cross section was performed both with and without using information from the VELO. Without the VELO information, the data are noisier and the mass resolution is worse, but the yields are significantly higher. For this measurement the trigger was open, so every collision was written to tape. The integrated luminosity of  $6.8\ \mu\text{b}^{-1}$  was determined by using beam-gas interactions measured with the VELO to profile the beam. There are three bins of rapidity  $y$  from 2.5 to 4.0, and eight bins of transverse momentum  $p_T$  from 0 to  $1.6\text{ GeV}/c$ . The results shown in fig. 3 agree reasonably well with Monte Carlo expectation, although it appears that the agreement with Perugia 0 may be slightly better than that with Pythia.

### 4. – Cross section for $b\bar{b}$ production at $\sqrt{s} = 7\text{ TeV}$

The measurement of the cross section for  $b\bar{b}$  production is an important test of theoretical predictions. Moreover, it is required to determine the sensitivity of LHCb to most new physics processes studied at the experiment. The cross section was measured using semileptonic  $B$  decays involving  $b \rightarrow D^0\mu^-\bar{\nu}$  [4]. Two analyses were performed, one with  $3\text{ nb}^{-1}$  of data taken with an open trigger, and one with  $11\text{ nb}^{-1}$  using muonic triggers.

Key steps in the analysis include the identification and removal of the prompt charm background, and the estimation of the efficiency of the muon triggers. The former is done using the logarithm of the impact parameter (IP) distribution, since in the ideal case  $D$  decays from the primary vertex (PV) should have zero IP. In practice the IP is nonzero due to the resolution of the detector, but it is generally much lower than the IP to the PV of  $D$  mesons from  $B$  decays. Therefore a two-dimensional log-likelihood fit to the mass of the  $D^0$  and the logarithm of its IP was performed. This allows simultaneous estimation of the background from prompt charm and that from other sources (combinatorics), which

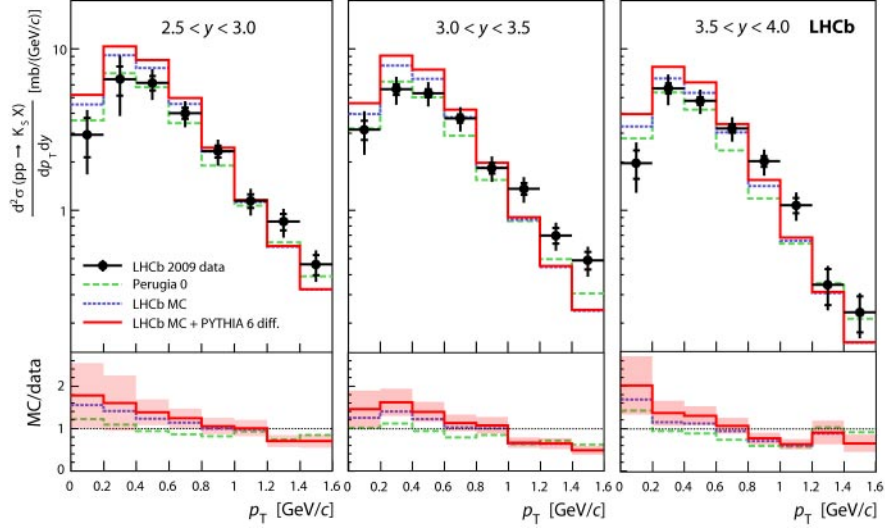


Fig. 3. – Cross section for prompt  $K_S^0$  production at  $\sqrt{s} = 0.9$  TeV [3].

would show up in the sidebands of the mass spectrum. The fits to the IP in the triggered sample are reproduced in fig. 4. In the “right-sign” decays the kaon and muon have the same charge; in the “wrong-sign” decays they have opposite charge.

The estimation of the trigger efficiency is carried out by comparing the number of prompt  $J/\psi \rightarrow \mu^- \mu^+$  decays in the open triggered sample which fired the muon trigger to those which did not. In the triggered dataset the number of these decays that were triggered independently of the single muon trigger is also studied. The trigger is found to be slightly more efficient than its simulation predicts. The results are presented in fig. 5 and compared to theory predictions. The Monte Carlo for Femtobarn Processes (MCFM) [5] and Fixed Order plus Next to Leading Log (FONLL) predictions [6] are both

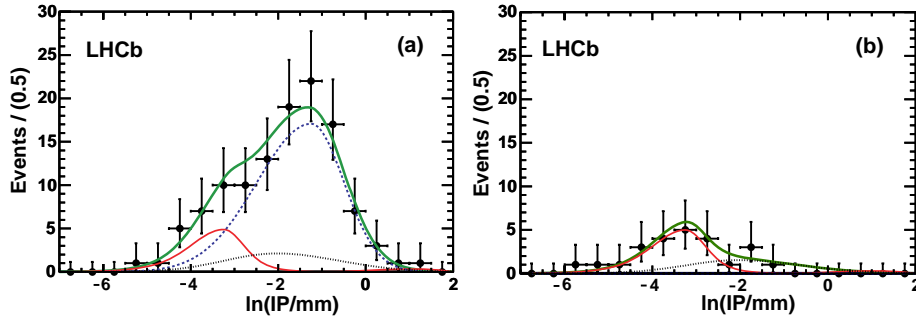


Fig. 4. – Impact parameter distributions for  $D$  decays to right-sign (left) and wrong-sign (right)  $K\pi$  combinations. The overall fit is shown by a thick solid line (green online), whilst the prompt charm background is shown by a thin solid line (red online), the dashed line is signal  $B$  decays to charm, and the dotted line is background from other sources.

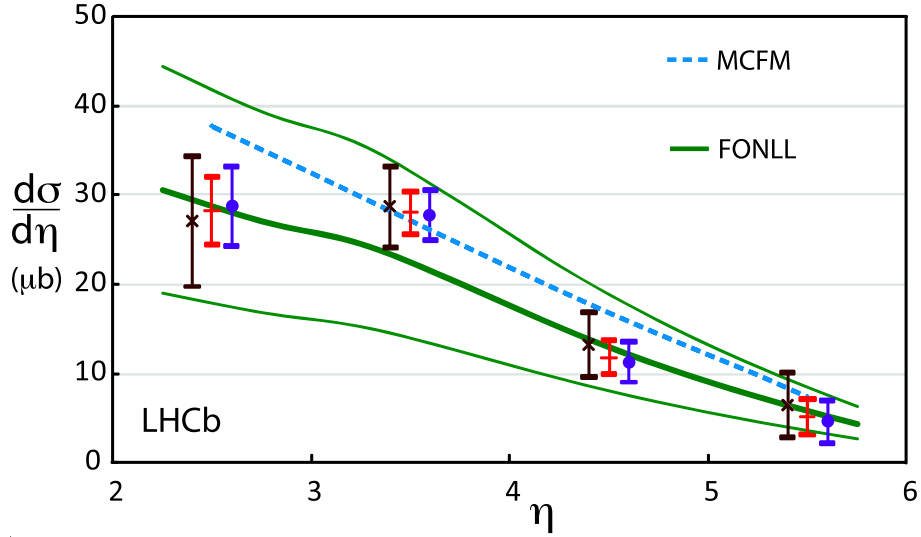


Fig. 5. – The  $b\bar{b}$  cross sections as a function of pseudorapidity  $\eta$ . The results obtained with an open trigger are marked with  $\times$ , the muon-triggered results with  $\bullet$  and the average with  $+$ . The thin lines (in green online) represent the theoretical uncertainty on the FONLL prediction.

based on next to leading order (NLO) calculations. However, the MCFM prediction is based on Martin-Stirling-Thorne-Watt (MSTW) parton density functions (PDFs) [7], whilst the FONLL prediction uses CTE6.5 PDFs and resums the  $p_T$  logarithms up to next to leading order [4]. There is a bin-independent systematic uncertainty on the experimental data of 17% that is primarily due to tracking efficiency and luminosity and is not shown on the plot. The overall cross section extrapolated into a  $4\pi$  detector acceptance is

$$(1) \quad \sigma(pp \rightarrow b\bar{b}X) = (284 \pm 20 \pm 49) \mu\text{b},$$

It is clear that the cross sections are in good agreement with expectations. They have since been used, for example, to determine the sensitivity of LHCb to the branching ratio of one of its flagship decay channels, the rare decay  $B_s^0 \rightarrow \mu^+\mu^-$ . This decay proceeds only via a penguin diagram, and is strongly suppressed: the Standard Model branching ratio is  $(3.35 \pm 0.32) \times 10^{-9}$ . At the time of writing the latest result from LHCb on this channel can be found in [8]. The cross section measurement is also key to determining the LHCb sensitivity to key  $CP$ -violating parameters such as the  $B_s^0$  oscillation phase  $\phi_s$ , which will be measured via a time-dependent angular analysis of the decay  $B_s^0 \rightarrow J/\psi\phi$  [9].

## 5. – Quarkonia

LHCb has also helped to shed light on various problems in the spectroscopy of quarkonia. For example, the cross section for prompt  $J/\psi$  production is not well modelled by either the colour singlet or colour octet models as implemented in the LHCb Monte Carlo. A measurement of this cross section has been performed [10]. The projection

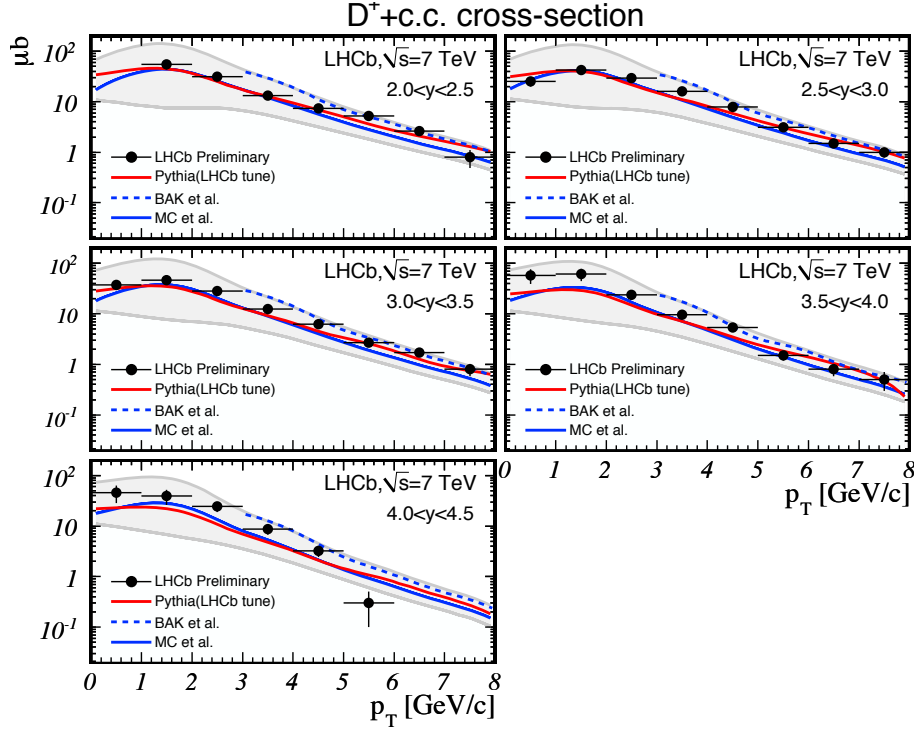


Fig. 6. – (Colour on-line) The  $D^+$  cross section in bins of  $p_T$  for five bins of  $y$ . The results are compared to the LHCb tune of Pythia, in red, and two other theoretical calculations. The region of the Pythia uncertainty is shaded in grey. There is a global correlated systematic uncertainty in the experimental data of 16% that is not shown on the plot.

of the lifetime in the  $z$ -direction is used to distinguish prompt  $J/\psi$  from  $J/\psi$  from  $B$  decays. The latter can be used to measure the  $b\bar{b}$  cross section as a check of the analysis of semileptonic  $B$  decays outlined in sect. 4. The result obtained is

$$(2) \quad \sigma(pp \rightarrow b\bar{b}X) = (288 \pm 4 \pm 48) \mu\text{b}$$

which agrees well with the  $(284 \pm 20 \pm 49) \mu\text{b}$  obtained previously. The most recent results for the prompt  $J/\psi$  cross section are obtained from a fit to the invariant mass distribution in  $0 < p_T < 14 \text{ GeV}$ ,  $2.5 < y < 4$  as  $(10.52 \pm 0.04 \pm 1.40^{+1.64}_{-2.20}) \mu\text{b}$ . The first uncertainty is statistical, the second is systematic, and the third is due to the unknown polarisation of the  $J/\psi$  (which is assumed to be zero). A measurement in bins of  $p_T$  is also performed.

## 6. – Open charm

Complementary to both  $b\bar{b}$  and charmonium production, the measurement of open charm production cross sections is an important step in LHCb's charm physics programme. The sensitivity to direct and indirect  $CP$  violation in charm decays depends on the  $c\bar{c}$  cross section. The measured production rate of  $c\bar{c}$  is about 20 times that of  $b\bar{b}$ , suggesting that high-statistics precision measurements in the charm sector have great potential at LHCb.

The charm production cross section was measured using similar techniques to the  $b\bar{b}$  analysis, but using exclusively hadronic decays [11]. The higher statistics available in open-triggered data allow separate measurements of  $D^0$ ,  $D^+$ ,  $D^*$  and  $D_s^+$  cross sections, with the  $\Lambda_c^+$  result to follow. The efficiency of the reconstruction and selection can be calculated from LHCb Monte Carlo, while calibration samples of  $K_s^0$ ,  $\phi$  and  $\Lambda$  are used to determine the particle identification efficiency. This data-driven technique was shown to work well, and will be crucial in future LHCb measurements. For example, the CKM angle  $\gamma$  can be determined via  $B \rightarrow DK$  decays with the ADS/GLW analysis methods [12, 13] given good knowledge of several ratios of branching fractions. These will depend strongly on the kaon identification efficiency [9].

As in the  $b\bar{b}$  measurement, the impact parameter distribution is used to separate charm from the proton-proton interaction from charm from  $B$  decays. The measurement is carried out in 5 bins of rapidity  $y$  and 8 bins of transverse momentum  $p_T$  (except for the  $D_s^+$  case where the statistics are insufficient and one-dimensional measurements in slices of  $p_T$  and  $y$  were performed separately). As an example the  $D^+$  results are reproduced in fig. 6. In the high-statistics modes it was confirmed that the trend in relative yield of prompt and secondary charm follows that in the LHCb Monte Carlo with individual fits to the IP distribution in each bin.

The dominant systematic uncertainties arise from the tracking efficiency and integrated luminosity. There are also systematic uncertainties associated with the fitting of mass and IP, and differences between data and Monte Carlo in variables used to select the sample. The results are largely in agreement with theoretical expectations.

Current analyses in the charm physics sector that will benefit from this study include measurements of the  $CP$ -violating parameters  $y_{CP}$  and  $A_\Gamma$ , the search for the rare decay  $D^0 \rightarrow \mu^+\mu^-$ , and a search for direct  $CP$  violation in the Dalitz plot of  $D^+ \rightarrow K^-K^+\pi^+$ .

## 7. – Outlook

The 2010 run has been very productive for all the LHC experiments. The LHC machine performed extremely well and the LHCb detector surpassed expectations, producing solid physics results in a challenging environment. In 2011 and 2012 we look forward to high-precision measurements of crucial Standard Model parameters such as the CKM angle  $\gamma$  and  $B_s$  oscillation phase, searches for very rare decays such as  $B_s^0 \rightarrow \mu^+\mu^-$ , searches for new physics in the charm sector, and many other exciting results.

\* \* \*

I would like to thank the organisers of the workshop for the opportunity to show these results.

## REFERENCES

- [1] AUGUSTO ALVES A. *et al.*, *JINST*, **3** (2008) S08005.
- [2] SPIRO M., *Proceedings of Science, ICHEP* (2010) 563.
- [3] AAIJ R. *et al.*, *Phys. Lett. B*, **693** (2010) 69.
- [4] AAIJ R. *et al.*, *Phys. Lett. B*, **694** (2010) 209.
- [5] NASON P., DAWSON S. and ELLIS R. K., *Nucl. Phys. B*, **303** (1988) 607.
- [6] CACCIARI M., FRIXIONE S., MANGANO M. L., NASON P. and RIDOLFI G., *JHEP*, **2004** (2004) 033.

- [7] MARTIN A. D., STIRLING W. J., THORNE R. S. and WATT G., *Eur. Phys. J. C*, **63** (2009) 189.
- [8] AAIJ R. *et al.*, *Phys. Lett. B*, **699** (2011) 330.
- [9] ADEVA B. *et al.*, *LHCb-PUB-2009-029* (2009).
- [10] AAIJ R. *et al.*, *Eur. Phys. J. C*, **71** (2011) 1645.
- [11] AAIJ R. *et al.*, *LHCb-CONF-2011-021* (2010).
- [12] ATWOOD D., DUNIETZ I. and SONI A., *Phys. Rev. Lett.*, **78** (1997) 3257.
- [13] GRONAU M. and LONDON D., *Phys. Lett. B*, **253** (1991) 483.